Published in final edited form as:
Science. 2011 December 2; 334(6060): 1278–1283. doi:10.1126/science.1211485.

Inhibition of pyruvate kinase M2 by reactive oxygen species contributes to cellular antioxidant responses

Dimitrios Anastasiou[1,2], **George Poulogiannis**[1,2], **John M. Asara**[1,3], **Matthew B. Boxer**[4], **Jian-kang Jiang**[4], **Min Shen**[4], **Gary Bellinger**[1,5], **Atsuo T. Sasaki**[1,2], **Jason W. Locasale**[1,2], **Douglas S. Auld**[4,§], **Craig J. Thomas**[4], **Matthew G. Vander Heiden**[5,6], and **Lewis C. Cantley**[1,2,*]

[1]Beth Israel Deaconess Medical Center, Department of Medicine-Division of Signal Transduction, Boston, MA 02115, USA

[2]Department of Systems Biology, Harvard Medical School, Boston, MA 02115, USA

[3]Department of Medicine, Harvard Medical School, Boston, MA 02115, USA

[4]NIH Chemical Genomics Center, National Human Genome Research Institute, National Institutes of Health, 9800 Medical Center Drive, Rockville, Maryland 20850, USA

[5]Koch Institute for Integrative Cancer Research at Massachusetts Institute of Technology Cambridge, MA 02139, USA

[6]Dana Farber Cancer Institute, Harvard Medical School, Boston, MA 02115, USA

Abstract

Control of intracellular reactive oxygen species (ROS) concentrations is critical for cancer cell survival. We show that, in human lung cancer cells, acute increases in intracellular concentrations of ROS caused inhibition of the glycolytic enzyme pyruvate kinase M2 (PKM2) through oxidation of Cys^{358}. This inhibition of PKM2 is required to divert glucose flux into the pentose phosphate pathway and thereby generate sufficient reducing potential for detoxification of ROS. Lung cancer cells in which endogenous PKM2 was replaced with the Cys^{358} to Ser^{358} oxidation-resistant mutant exhibited increased sensitivity to oxidative stress and impaired tumor formation in a xenograft model. Besides promoting metabolic changes required for proliferation, the regulatory properties of PKM2 may confer an additional advantage to cancer cells by allowing them to withstand oxidative stress.

Control of the intracellular concentrations of reactive oxygen species (ROS) is critical for cell proliferation and survival. In cells treated with growth factors, transient increases in ROS concentrations are implicated in enhanced cell proliferation through inhibition of phosphotyrosine phosphatases and PTEN, allowing amplification of tyrosine kinase and phosphatidylinositol-3 kinase (PI-3K) signaling pathways (1). However, high concentrations of ROS can also damage cellular components and compromise cell viability (2). Tumor suppressor and oncogenic pathways frequently mutated in cancer commonly result in increased accumulation of ROS (3–7). Furthermore, conditions associated with tumorigenesis such as hypoxia, matrix detachment, mitochondrial dysfunction and inflammation can all lead to excess production of ROS (8–12). Therefore, cancer cells are particularly challenged in dealing with oxidative stress (2, 13).

*Corresponding author: Lewis C. Cantley, Harvard Medical School, 3 Blackfan Circle, CLS 412, Boston, MA 02115, USA, Tel: +1 617 735 2601, Fax: +1 617 735 2646, lewis_cantley@hms.harvard.edu.
§Current address: Novartis Institutes for Biomedical Research, Center for Proteomic Chemistry, Cambridge, MA 02139, USA.

Detoxification of ROS and the repair of oxidatively damaged proteins depend primarily on the availability of reduced glutathione (GSH). Glucose metabolism through the pentose phosphate pathway provides NADPH to maintain glutathione in the reduced state (14, 15). Glucose is also a major carbon source for biosynthetic processes (16). How glucose is metabolized in cancer cells is determined, in part, by expression of the glycolytic enzyme pyruvate kinase M2 (PKM2) (17). In contrast to its splice variant PKM1, which is expressed in many adult tissues, PKM2 is allosterically activated in a feed-forward regulatory loop by an upstream glycolytic metabolite, fructose-1,6-bisphosphate (FBP) and is susceptible to inhibition by growth factor signaling through interaction with phosphotyrosine-containing proteins (18). These properties of PKM2 allow proliferating cells to divert glucose into anabolic pathways emanating from glycolysis in order to meet the increased biosynthetic demands of proliferation.

Pyruvate kinase (PK) orthologues in many organisms, from bacteria to humans, are inhibited by oxidants (19–22). Exposure of A549 human lung cancer cells to 1 mM H2O2, 250 μM diamide (a thiol-oxidizing compound), or hypoxia (1% O_2) [which causes increased ROS production by mitochondrial complex III (23)], resulted in similar increases in intracellular concentrations of ROS (fig. S1) and caused decreases in PKM2 activity (Fig. 1A and B) (24). In all cases, incubation of cell lysates with dithiothreitol (DTT), a strong reducing agent, restored PKM2 activity to nearly that of untreated cells, indicating that the effects of treating cells with diamide, H_2O_2 or hypoxia on PKM2 activity reflect an oxidative event that is reversible with a thiol reducing agent.

Association of PKM2 subunits into homotetramers is required for optimal enzymatic activity (25). Diamide treatment impaired co-immunoprecipitation of endogenous PKM2 with Flag-tagged PKM2 and this was reversed by adding DTT to the cell lysates prior to immunoprecipitation (Fig. 1C). These results indicate either that oxidative stress induces PKM2 subunits to dissociate *in vivo* or that it makes subunit association less stable during cell lysis and immunoprecipitation. In either event, this change in association of PKM2 subunits after diamide treatment correlated with decreased enzymatic activity.

We examined whether diamide treatment differentially affected PKM2 versus PKM1 activity by assaying pyruvate kinase activity in lysates from cells engineered to express equivalent amounts of either Flag-PKM1 or Flag-PKM2 with concomitant depletion of endogenous PKM2 by shRNA (henceforth referred to as Flag-PKM1/kd cells or Flag-PKM2/kd cells, respectively; kd: knock-down). Unlike that of PKM2, the activity of PKM1 did not change following diamide treatment (Fig. 1D). Consistent with this observation, formation of complexes between Flag-PKM1 and endogenous PKM2 (using cells still expressing endogenous PKM2) was unaffected by diamide (Fig. 1E). This result suggests that the hetero-multimer of PKM1 and PKM2 is protected from oxidation-dependent destabilization.

To assess a possible covalent modification of PKM2, we treated A549 cells with or without diamide and subjected cell lysates to SDS-polyacrylamide gel electrophoresis (PAGE) under non-reducing conditions. Subsequent protein immuno-blot analysis revealed that some PKM2 from diamide-treated cells migrated faster (Fig. 2A, upper panel). This faster-migrating form was not observed when SDS-PAGE was done under reducing conditions (Fig. 2A, lower panel). Cysteine residues are particularly prone to oxidation because the sulfhydryl group reacts with various oxygen species, and this reactivity can be influenced by the local protein microenvironment (26). Structural analysis of PKM2 revealed three cysteine residues that could affect subunit interaction, enzymatic activity, or both. Cys^{31} and Cys^{424} are located at the subunit interaction interface whereas Cys^{358} is located in a beta barrel that includes residues essential for catalytic activity (fig. S2A–B) (27). Substitution of

Cys^{358} with Ser^{358} (C358S) abrogated the faster-migrating PKM2 band (Fig. 2B, upper panels), but mutation of Cys^{31} or Cys^{424} did not (fig. S2C).

Lysis of cells under denaturing conditions in the presence of maleimide to block reduced cysteines in proteins, followed by reduction of oxidized cysteines and labeling with biotin-maleimide allows the detection of oxidized proteins with streptavidin (24). Using this method, we detected biotin-labeled Flag-PKM2 in lysates of diamide-treated cells but not in those of control cells (Fig. 2B, lower panels). In contrast, we did not detect biotinylated Flag-PKM2(C358S). Furthermore, unlike Flag-PKM2, Flag-PKM2(C358S) still associated with endogenous PKM2 after diamide treatment (Fig. 2C) and the enzymatic activity of the C358S mutant was less sensitive to oxidant-induced inhibition (Fig. 2D). These results indicate that although oxidation of other Cys residues in PKM2 may have minor effects on PKM2 catalytic activity, oxidation of Cys^{358} primarily accounts for ROS-induced inactivation.

Small molecule activators selectively increase the activity of PKM2 with no effects on PKM1 (28). Treatment of purified recombinant PKM2 with the small molecule PKM2 activator DASA-10 (NCGC00181061, a substituted *N,N′*-**di**ary**l**sulfon**a**mide, fig. S3A) prevented inhibition of PKM2 by H_2O_2 (fig. S3B). Incubation of A549 cells with 20 μM DASA-10 caused a 2.8-fold increase in enzyme activity in the absence of diamide, and prevented the diamide-induced inhibition of PKM2 activity (fig. S3C and Fig. 2E). Furthermore, DASA-10 preserved the co-precipitation of endogenous PKM2 with Flag-PKM2 after treatment of cells with diamide (Fig. 2F). Addition of DASA-10 after lysis of diamide-treated cells was less effective in restoring PKM2 activity (fig. S3D). The activator likely maintains PKM2 in an active conformation and thus prevents oxidation of Cys^{358}; however, PKM2 oxidation before addition of activator impairs the ability of the activator to increase the enzymatic activity of PKM2. Likewise, despite the presence of Cys^{358} in PKM1, the failure of this isoform to be inhibited by diamide (Fig. 1D), could be explained by residues in PKM1 that stabilize the active tetramer and thereby block access of ROS to Cys^{358}.

To gain insights into the functional consequences of PKM2 inhibition under oxidative stress, we investigated changes in cellular metabolism following diamide treatment in the presence or absence of DASA-10 (fig. S4). We monitored flux of glucose into the pentose phosphate pathway (PPP), which produces NADPH for ROS detoxification (14, 15, 29). Diamide treatment stimulated PPP-dependent $^{14}CO_2$ production from [1-^{14}C]-glucose (p=0.02) in A549 cells (Fig. 3A) indicating that flux into the oxidative branch of the PPP was enhanced in response to oxidative stress (15, 29). In the presence of DASA-10, diamide did not cause a significant increase in PPP-specific $^{14}CO_2$ production (Fig. 3A), suggesting that ROS-dependent inhibition of PKM2 is needed to maintain the availability of glucose-6-phosphate (G-6-P) for flux into the PPP. Consistent with this idea, after 30 minutes of diamide treatment, the cellular concentration of G-6-P increased 2.3-fold (Fig. 3B). Although this could be a consequence of inhibiting any step in glycolysis or from stimulation of glucose uptake and phosphorylation, the concentration of G-6-P decreased 75.5±17.6% when PKM2 inhibition by diamide was prevented by the presence of DASA-10 (Fig. 3B), indicating that ROS-induced inhibition of PKM2 may account for the accumulation of G-6-P in response to oxidative stress.

Glucose catabolism via the PPP provides NADPH required for glutathione reductase to generate GSH for ROS detoxification. Cells expressing Flag-PKM2(C358S) in the absence of endogenous PKM2 [henceforth referred to as Flag-PKM2(C358S)/kd cells] had lower amounts of GSH than Flag-PKM2/kd cells (Fig. 3C, left). Similarly, treatment of parental cells with either DASA-10 (Fig. 3C, right) or another structurally related PKM2 activator,

DASA-58 (NCGC00185916, ML203, fig. S3A & S5A) resulted in lower amounts of GSH. This decrease in GSH concentration was not observed in Flag-PKM1/kd cells even after longer periods of activator treatment (fig. S5B). Because PKM1 activity is unaffected by DASA-10 or DASA-58 (28), these results indicate that the effects of these compounds on GSH concentration are a consequence of PKM2 activation, rather than off-target effects.

To test whether decreased abundance of GSH induced by the PKM2 activators impaired cellular capacity for ROS detoxification, we measured intracellular ROS concentrations after treatment of cells with H_2O_2. H_2O_2 elicited greater accumulation of ROS in PKM2 activator-treated cells than in DMSO-treated cells, and this difference was more pronounced with increased amounts of H_2O_2 (Fig. 3D and fig. S5C). Genetic replacement of PKM2 with PKM1 in mouse embryo fibroblasts (MEFs) (fig. S6 A & B) resulted in increased accumulation of ROS in H_2O_2-treated cells compared to that in MEFs with intact PKM2 (fig. S6C). Thus, PKM2 inhibition due to oxidative stress contributes to a metabolic response that can deplete ROS.

To test whether this mechanism is relevant for cell survival under oxidative stress, we examined the effects of DASA-10 on diamide- or H_2O_2-induced cell death. In response to treatment with either H_2O_2 or diamide, cell death was increased in PKM2 activator-treated cells compared to DMSO-treated cells (Fig. 4A & fig. S7). Also, Flag-PKM2(C358S)/kd cells were more sensitive to diamide than Flag-PKM2/kd cells (Fig. 4B).

We monitored cell mass accumulation of Flag-PKM2/kd or Flag-PKM2(C358S)/kd cells over several days in an atmosphere of 21% or 1% oxygen to determine whether PKM2 inhibition under conditions of increased endogenous ROS levels induced by hypoxia (fig. S1) was functionally relevant. With standard tissue culture concentrations of glucose (25 mM), the proliferation of the two cell-lines was indistinguishable at either 21% oxygen (fig. S8 A&B) or 1% oxygen (fig. S8C). In contrast, when the glucose concentration in the media was reduced to a physiological level of 5.6 mM, Flag-PKM2(C358S)/kd cells showed a modest but reproducible (p=0.0041) decrease in cell mass accumulation (fig. S8D). This was more evident when cells were grown in 1% oxygen (Fig. 4C). Under the same culture conditions, we could detect oxidation of endogenous PKM2 which was diminished when cells were treated with the anti-oxidant N-acetyl-cysteine (NAC) (fig. S9A). In contrast, we detected neither biotin-maleimide labeling (fig. S9B), nor a significant change in the enzymatic activity of Flag-PKM2(C358S) under hypoxia (fig. S9C). These data indicate that the C358S mutant is refractory to hypoxia-induced oxidation. When the cell-permeable GSH analogue glutathione-monoethylester (GSH-MEE) was present in the medium for the duration of the experiment, there was no difference in cell mass accumulation between Flag-PKM2(C358S)/kd cells and Flag-PKM2(WT)/kd cells (Fig. 4D). Furthermore, a phosphotyrosine-containing peptide with amino acid sequence corresponding to the optimal PKM2 binding motif (18) inhibited the activities of both Flag-PKM2 and Flag-PKM2(C358S) to a similar degree (fig. S9D) suggesting that the impaired proliferation of Flag-PKM2(C358S)/kd cells is unlikely to be a result of differential sensitivity to growth factor inhibition of the C358S mutant relative to that of PKM2(WT). Therefore, the diminished proliferation of Flag-PKM2(C358S)/kd cells appears to result from impaired antioxidant capacity. Inhibition of PKM2 after oxidative stress contributes to sustaining cell survival when endogenous ROS accumulate.

To determine whether the proposed role for PKM2 in survival under oxidative stress is relevant *in vivo*, we injected cells into immunocompromised (*nu/nu*) mice and assayed formation of tumors (fig. S10A). Half the mice were given access to standard water and half to water containing NAC throughout the experiment. Tumors derived from Flag-PKM2(C358S)/kd cells were significantly (p=0.011) smaller compared to those expressing

wild-type Flag-PKM2 (Fig. 4E and fig. S10). This difference in tumor growth was alleviated in mice treated with NAC. Thus, regulation of PKM2 via oxidation of Cys^{358} is critical under these conditions for optimal tumor growth.

Cancer cells experience a substantial need for providing reducing power in the form of NADPH to fuel biosynthesis of lipids and nucleotides that are in high demand during proliferation (16). Consequently, under conditions of oxidative stress, NADPH supply must be appropriately enhanced in order to sustain proliferation while maintaining ROS homeostasis through GSH. Our data indicate that, besides metabolic reprogramming functions associated with promoting anabolic processes, expression of a specific pyruvate kinase isoform, PKM2, confers additional advantages to cancer cells by allowing them to sustain anti-oxidant responses and thereby support cell survival under acute oxidative stress. As increasing PKM2 activity would compromise both its pro-anabolic and anti-oxidant functions, the use of small molecule PKM2 activators may be an appropriate approach to interfere with cancer cell metabolism for therapeutic purposes.

Supplementary Material

Refer to Web version on PubMed Central for supplementary material.

Acknowledgments

We thank: V. Toxavidis and J. Tigges (BIDMC Flow Cytometry Facility) for support with flow cytometry applications; X. Yang and S. Breitkopf for technical assistance with mass spectrometry; Ross Dickins and Scott Lowe (CSHL) for the gift of tamoxifen-inducible Cre-expressing retroviral plasmid; C. Benes, N. Wu, A. Shaywitz, B. Emerling, A. Saci, G. DeNicola, K. Courtney, A. Couvillon, S. Soltoff, A. Carracedo, A. Grassian, J. Brugge, and members of the Cantley lab for helpful discussions. L.C.C. is a co-founder of Agios Pharmaceuticals, a company that seeks to develop novel therapeutics which target cancer metabolism. G.P. is a Pfizer fellow of the Life Sciences Research Foundation. A.T.S. is a Genentech fellow and supported by the Japanese Society for the Promotion of Science and the Kanae Foundation for Research Abroad. M.V.H. is supported by the NIH (R03MH085679 & 1P30CA147882), the Burroughs Wellcome Fund, the Damon Runyon Cancer Research Foundation and the Smith Family. This work was supported by grants from the NIH (R01-GM056203-13, P01-CA089021 & P01- CA117969-04 to L.C.C), the Starr Cancer Consortium (L.C.C. and M.V.H.), the Molecular Libraries Initiative of the National Institutes of Health Roadmap for Medical Research and the Intramural Research Program of the National Human Genome Research Institute, National Institutes of Health (M.B.B, J.-k. J., M.S., D.S.A. and C.J.T.). We apologize to colleagues whose work we could not cite due to space limitations.

References and Notes

1. Tonks NK. Cell. 2005; 121:667. [PubMed: 15935753]
2. Wellen KE, Thompson CB. Mol Cell. 2010; 40:323. [PubMed: 20965425]
3. Vafa O, et al. Mol Cell. 2002; 9:1031. [PubMed: 12049739]
4. Nogueira V, et al. Cancer Cell. 2008; 14:458. [PubMed: 19061837]
5. Sablina AA, et al. Nat Med. 2005; 11:1306. [PubMed: 16286925]
6. Bensaad K, Cheung EC, Vousden KH. EMBO J. 2009; 28:3015. [PubMed: 19713938]
7. Hu W, et al. Proc Natl Acad Sci U S A. 2010; 107:7455. [PubMed: 20378837]
8. Reuter S, Gupta SC, Chaturvedi MM, Aggarwal BB. Free Radic Biol Med. 2010; 49:1603. [PubMed: 20840865]
9. Halliwell B. Biochem J. 2007; 401:1. [PubMed: 17150040]
10. Schafer ZT, et al. Nature. 2009; 461:109. [PubMed: 19693011]
11. Ishikawa K, et al. Science. 2008; 320:661. [PubMed: 18388260]
12. Weinberg F, et al. Proc Natl Acad Sci U S A. 2010; 107:8788. [PubMed: 20421486]
13. Levine AJ, Puzio-Kuter AM. Science. 2010; 330:1340. [PubMed: 21127244]
14. Pandolfi PP, et al. EMBO J. 1995; 14:5209. [PubMed: 7489710]
15. Filosa S, et al. Biochem J. 2003; 370:935. [PubMed: 12466018]

16. Vander Heiden MG, Cantley LC, Thompson CB. Science. 2009; 324:1029. [PubMed: 19460998]
17. Christofk HR, et al. Nature. 2008; 452:230. [PubMed: 18337823]
18. Christofk HR, Vander Heiden MG, Wu N, Asara JM, Cantley LC. Nature. 2008; 452:181. [PubMed: 18337815]
19. Maeba P, Sanwal BD. J Biol Chem. 1968; 243:448. [PubMed: 4865644]
20. McDonagh B, Ogueta S, Lasarte G, Padilla CA, Barcena JA. J Proteomics. 2009; 72:677. [PubMed: 19367685]
21. Butterfield DA, Sultana R. J Alzheimers Dis. 2007; 12:61. [PubMed: 17851195]
22. Cumming RC, et al. J Biol Chem. 2004; 279:21749. [PubMed: 15031298]
23. Brunelle JK, et al. Cell Metab. 2005; 1:409. [PubMed: 16054090]
24. Information on materials and methods is available on Science Online.
25. Eigenbrodt E, Reinacher M, Scheefers-Borchel U, Scheefers H, Friis R. Crit Rev Oncog. 1992; 3:91. [PubMed: 1532331]
26. Janssen-Heininger YM, et al. Free Radic Biol Med. 2008; 45:1. [PubMed: 18423411]
27. Dombrauckas JD, Santarsiero BD, Mesecar AD. Biochemistry. 2005; 44:9417. [PubMed: 15996096]
28. Boxer MB, et al. J Med Chem. 2010; 53:1048. [PubMed: 20017496]
29. Le Goffe C, et al. Biochem J. 2002; 364:349. [PubMed: 12023877]

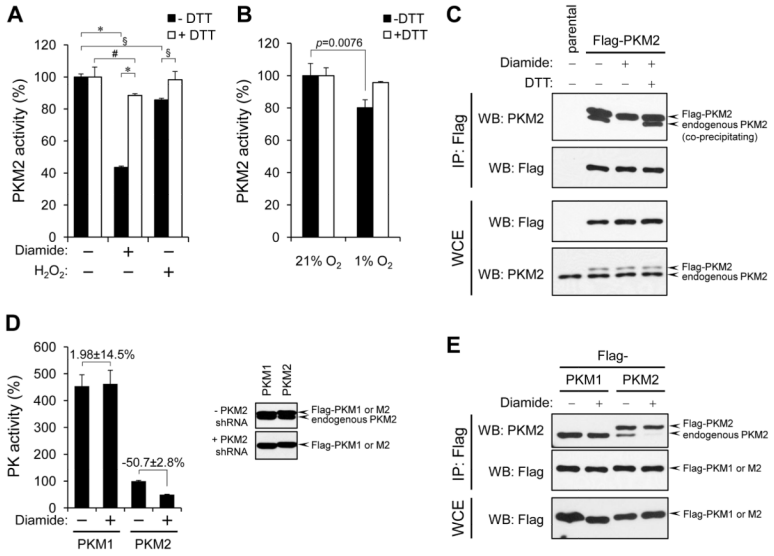

Figure 1. ROS-promoted dissociation of PKM2 subunits and inhibition of enzymatic activity

(A) A549 human lung cancer cells were treated with 250 μM diamide or 1mM H_2O_2 for 15 min. After cell lysis pyruvate kinase activity was assayed in the presence or absence of DTT. % PKM2 activity (mean ± SD) relative to untreated cells for each condition is shown (: $p<0.001$, §: $p<0.01$, #: $p<0.05$, 2-way ANOVA with Bonferroni post-tests, $N=3$).

(B) A549 cells were cultured in medium containing 5.6 mM glucose for 3 hours under 21% O_2 or 1% O_2. After cell lysis, PKM2 activity was assayed as in (A) (Student's t-test, $N=3$).

(C) A549 cells were engineered to express Flag-PKM2 (arrows). Cells were left untreated or were diamide-treated as in (A) and equal portions of lysates prepared under non-reducing conditions were supplemented or not with DTT (1 mM final concentration). Lysates were then subjected to immunoprecipitation with anti-Flag agarose beads in the presence or absence of DTT, followed by SDS-PAGE and western blot.

(D) A549 cells expressing Flag-PKM1 or Flag-PKM2 in the absence of endogenous PKM2 (referred to in the text as Flag-PKM1/kd or Flag-PKM2/kd) were generated as in (17). Expression of Flag-tagged proteins and depletion of endogenous PKM2 were confirmed by western blot with an antibody recognizing both PKM1 and PKM2 (right panel). Left panel: lysates of diamide-treated (250 μM, 15 min.) cells were prepared and assayed for pyruvate kinase activity as in (A). % pyruvate kinase activity (mean ± SD) for each condition relative to untreated Flag-PKM2/kd cells is shown. Numbers denote % difference in PK activity ± SD between diamide-treated versus non-treated Flag-PKM1/kd or Flag-PKM2/kd cells, respectively.

(E) A549 cells expressing Flag-PKM1 or Flag-PKM2 were treated with diamide (250 μM, 15 min.) and, after cell lysis, immunoprecipitation to assess the amount of endogenous PKM2 associated with the tagged PKM isoforms was performed as in (C).

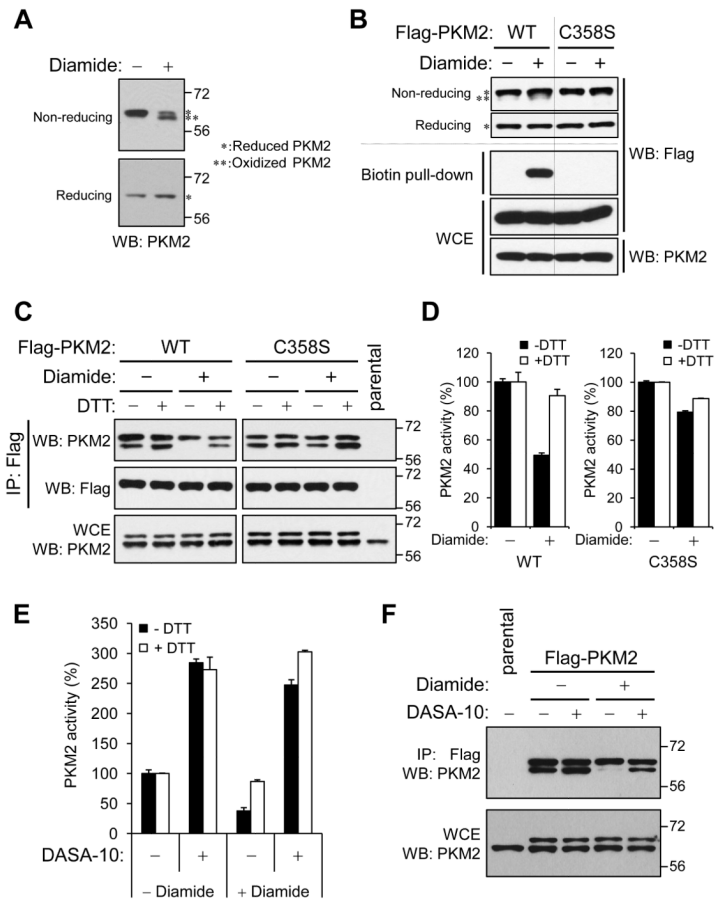

Figure 2. Protection of PKM2 from ROS-induced inhibition by substitution of Cys^{358} with Ser^{358} or by small molecule PKM2 activators

(A) A549 cells were treated with 1mM diamide for 15 min., lysed and analyzed by SDS-PAGE under reducing (lower panel) or non-reducing (upper panel) conditions. Asterisks throughout the figure mark bands corresponding to reduced PKM2 (*) or oxidized (**) PKM2.

(B) Upper panel: A549 cells expressing Flag-PKM2 or Flag-PKM2(C358S) were treated with 250 μM diamide for 15 minutes, lysed, and analyzed by SDS-PAGE under reducing or non-reducing conditions. Lower panel: A549 Flag-PKM2/kd or Flag-PKM2(C358S)/kd cells were treated with diamide as above. Oxidized proteins were labeled with biotin-maleimide (24), purified with streptavidin-sepharose beads and probed for the presence of Flag-PKM2 or Flag-PKM2(C358S) with Flag antibody.

(C) A549 cells expressing Flag-PKM2 or Flag-PKM2(C358S), were treated with 250 μM diamide for 15 min., lysed without DTT and split into equal portions that were supplemented with or without DTT (1 mM final concentration). After immunoprecipitation with anti-Flag agarose, immunoprecipitates were analyzed by reducing SDS-PAGE and western blot with the indicated antibodies.

(D) A549 Flag-PKM2/kd or Flag-PKM2(C358S)/kd cells were treated with diamide as in (C) and pyruvate kinase activity was assayed in cell lysates in the presence or absence of 1 mM DTT. % PKM2 activity (mean ± SD) relative to untreated cells for each condition is shown.

(E) Medium containing 20 μM PKM2 activator DASA-10 (28) was added to A549 cells at t=−1h; diamide was then added directly to the media at a final concentration of 250 μM at t=

−15 min. Cells were harvested at t=0, lysed, and pyruvate kinase activity in lysates was assayed in the presence or absence of 1 mM DTT. PKM2 activity is shown as in (D). **(F)** A549 cells expressing Flag-PKM2 were treated with DASA-10 and diamide as in (E) and the respective lysates were subjected to immunoprecipitation with anti-Flag agarose under non-reducing conditions. Immunoprecipitates were analyzed by reducing SDS-PAGE followed by western blot with a PKM2 antibody.

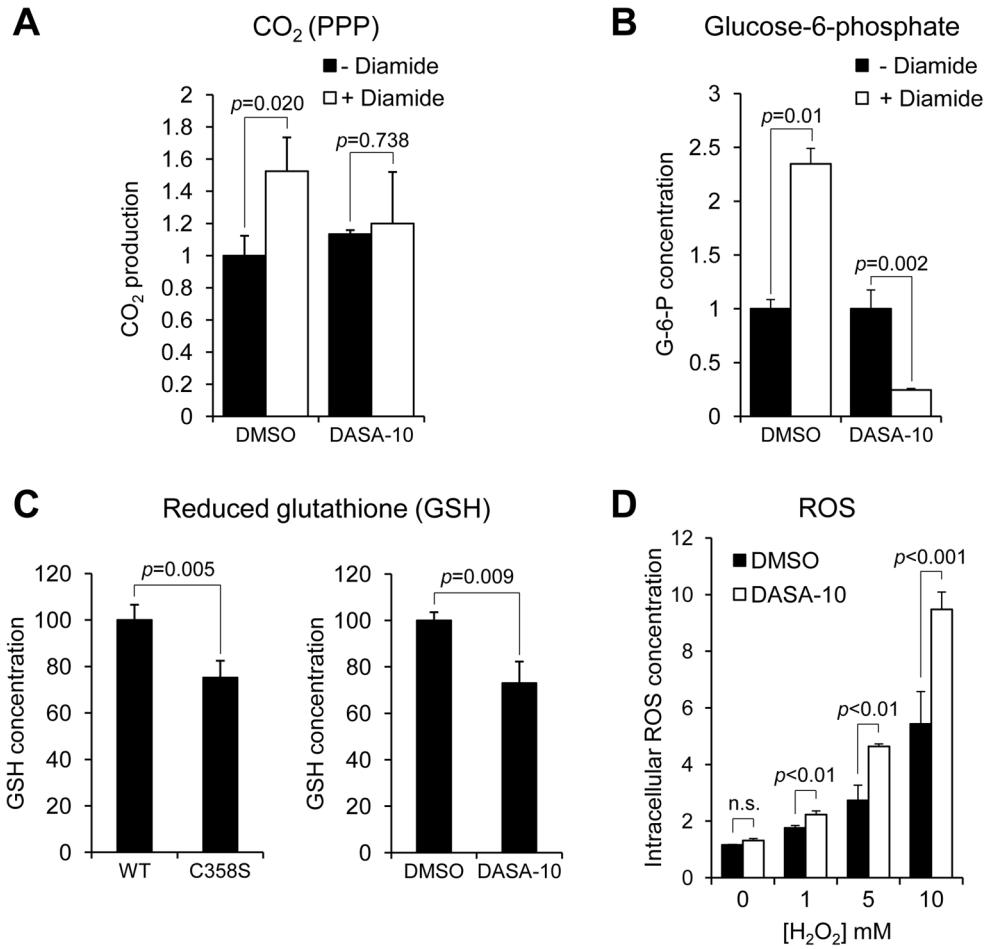

Figure 3. Changes in glucose metabolism required for cellular antioxidant responses are supported by ROS-induced inhibition of PKM2

(A) PPP-dependent glucose oxidation to CO_2. A549 cells were seeded and, after 24 hours, media were supplemented with [1-^{14}C]-glucose or [6-^{14}C]-glucose plus 10 μM DASA-10 and 100 μM diamide where indicated. Released $^{14}CO_2$ was measured after a 3-hour incubation of cells with labeled glucose. The rate of $^{14}CO_2$ production from glucose via the PPP was calculated as described (24). Mean PPP-dependent $^{14}CO_2$ release rates relative to (DMSO, - Diamide) ± SD are shown (Student's t-test, *N*=3).

(B) A549 cells were treated with 10 μM PKM2 activator DASA-10 or DMSO for 1 hour prior to addition of 250 μM diamide directly into the medium. Cellular metabolites were harvested at t=30 min. and analyzed by liquid chromatography coupled to triple quadrupole tandem mass spectrometry (LC-MS/MS) (24). Bars represent mean concentrations of glucose-6-phosphate at t=30 min. relative to t=0 min. ± SD (*N*=3). Statistical analysis details are described in (24).

(C) Intracellular GSH concentrations of A549 Flag-PKM2/kd and Flag-PKM2(C358S)/kd cells (left panel) or A549 cells treated either with PKM2 activator DASA-10 (10 μM) or DMSO for 1 hour (right panel) were assessed using ThiolTracker™ Violet. Mean GSH concentrations relative to WT or DMSO-treated cells, respectively, are shown (Student's *t*-test, *N*=3).

(D) After treatment with DMSO or 10 μM PKM2 activator DASA-10 for 1 h, A549 cells were incubated with the ROS-sensitive fluorescent dye CM-H_2DCFDA and H_2O_2 was added at the indicated concentrations. Cells were then collected after 15 minutes and ROS-

dependent fluorescence was measured by flow cytometry. Mean fluorescence intensities ± SD are shown and *p* values were calculated by 2-way ANOVA with Bonferroni post-tests (*N*=3).

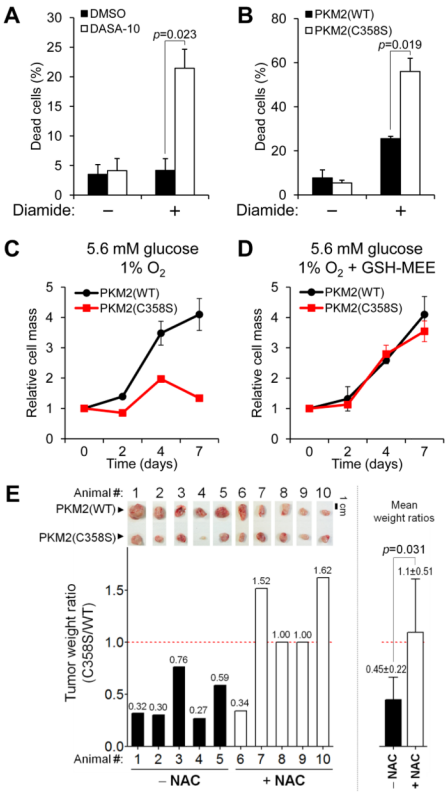

Figure 4. Promotion of cancer cell survival and tumor growth under oxidative stress by PKM2 inhibition

(A) DASA-10 (10 μM) or DMSO was added to H1299 human lung cancer cells at t=−1h. At t=0, 150 μM diamide was added directly into the medium. At t=+3h, cells were collected by trypsinization and stained with propidium iodide (PI). Dead (PI-stained) cells were scored by flow cytometry (Student's *t*-test, *N*=3).

(B) H1299 Flag-PKM2/kd or H1299 Flag-PKM2(C358S)/kd cells were treated with 150 μM diamide for 3 hours, at which point dead cells were detected as in (A) (Student's *t*-test, *N*=3).

(C and D) H1299 Flag-PKM2/kd or H1299 Flag-PKM2(C358S)/kd cells were seeded in medium containing 5.6 mM glucose and cultured in 1% oxygen (O_2) in the absence (C) or presence (D) of 4 mM glutathione monoethyl ester (GSH-MEE). Cells were fixed at the indicated time points and cell mass was quantified by crystal violet staining (C: $p<0.0001$, 2-way ANOVA, *N*=3) (24).

(E) Equal numbers of H1299 Flag-PKM2/kd or Flag-PKM2(C358)/kd cells were injected into the left and right flanks, respectively, of immunocompromised mice. Half had access to normal water and the other half to water supplemented with 40 mM NAC throughout the experiment. Upper panel: photographs of dissected tumors in pairs. The bar graphs represent tumor weight ratios with corresponding value above each bar (left) and mean weight ratios ± SD (right) (*p* value calculated by Student's t-test).